

Optical Properties of CdS_{0.2}Se_{0.8}:V

JONATHAN T. GOLDSTEIN,^{1,4} MELVIN OHMER,¹ S.M. HEGDE,¹
RAVINDRA PANDEY,² ARNOLD BURGER,³ STEVEN H. MORGAN,³
KUO-TONG CHEN,³ and YING-FANG CHEN³

1.—Air Force Research Lab., AFRL/MLPSO, Wright Patterson Air Force Base, Dayton, OH 45433.
2.—Michigan Technical University, Houghton, MI 49931. 3.—Department of Physics, Fisk
University, Nashville, TN 37208. 4.—E-mail: Jonathan.Goldstein@wpafb.af.mil

We report here a comparison between two methods for calculating the index of refraction of the CdS_xSe_{1-x} alloy system and a calculation of the phase-matching angles for second harmonic generation for this system. Analytical expressions for the index and the birefringence of all x values are presented. The low-temperature photoluminescence spectrum has been measured and reveals a native defect at 1.45 eV and a peak at 1.8 eV caused by the vanadium dopant, as well as an exciton peak at 2.24 eV. The transmission spectrum displays three peaks due to the vanadium dopant at 0.979 eV, 1.087 eV, and 1.181 eV. The birefringence has been measured for x = 0.2 from 1 μm to 14 μm and varies from 0.0185 to 0.0125.

Key words: CdS_xSe_{1-x}, vanadium, birefringence, phase matching

INTRODUCTION

Single-crystal CdSe has found extensive application as an optical-parametric oscillator (OPO).¹⁻¹¹ Alloying with S should be an effective method of extending the range over which this material is non-critically phase matchable. In addition to its function as an OPO, another interesting property of the CdS_xSe_{1-x} has recently come to light. The addition of vanadium has been shown to increase the photorefractive response of CdS_{0.2}Se_{0.8}:V to an extent that it is comparable with values of the best available materials.^{12,13} However, no studies of the CdS_{0.2}Se_{0.8}:V system's basic optical properties have been undertaken in over 20 years.¹⁴⁻¹⁷ We have, therefore, decided to investigate some of the basic properties relevant to the material's nonlinear applications, namely, its birefringence, photoluminescence, and the impurity-band absorption of the vanadium dopant.

THE INDEX OF REFRACTION OF THIS ALLOY SYSTEM

The mid-infrared refractive indices of CdS and CdSe have been reported by a number of authors.^{8,18-22} The agreement between the different reported values is quite excellent, as can be seen

throughout Fig. 1. Data for the indices of CdS_xSe_{1-x} alloys have been reported by Lisitsa et al.,²¹ who found indices for x = 0, 0.36, 0.58, 0.79, and 100. Using Lisitsa's data, we found that there is a linear relationship between the average index of refraction (the average of n_e and n_o) for a particular wavelength and alloy composition. The family of such linear curves for several wavelengths is presented in Fig. 2. The straight lines of Fig. 2 demonstrate the linear relationship

$$n_{\lambda} = mx + b \quad (1)$$

where n_λ is the index at a particular wavelength, and x is alloy composition, is an accurate representation of this material system. By fitting m and b to 100 such lines, we found empirically that

$$m(\lambda) = -\frac{1.39058 \lambda^3}{(\lambda^3 - 0.03633)} + 1.22499 \exp(-0.00349\lambda) \quad (2)$$

and

$$b(\lambda) = \frac{2.48276 \lambda^3}{(\lambda^3 - 0.03516)} - 0.01485 \exp(0.09953\lambda) \quad (3)$$

The results of using this method to estimate the alloy index largely overlap the more commonplace method of taking a weighed average of the coefficients

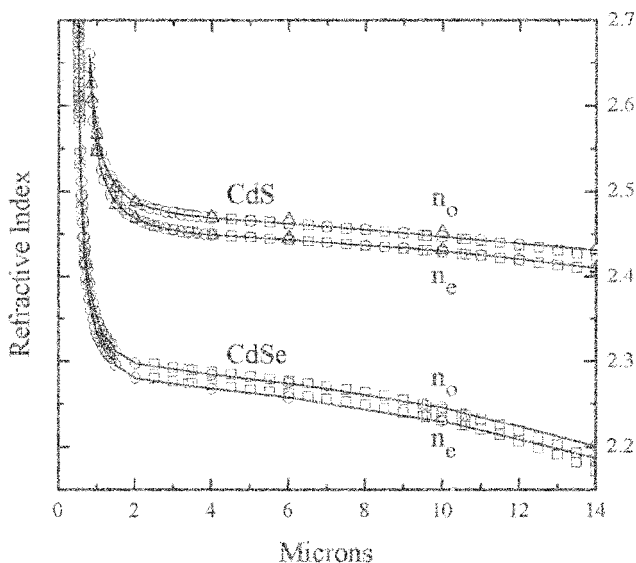


Fig. 1. The indices of refraction of the ordinary and extra-ordinary rays of CdS and CdSe, as reported by: \square Chenault, \circ Nikogosyan, and \triangle Piller [8, 18–22]. The straight line has been added as a visual aid. The agreement between the data from the different authors is such that the data sets essentially overlap out to 11 μm .

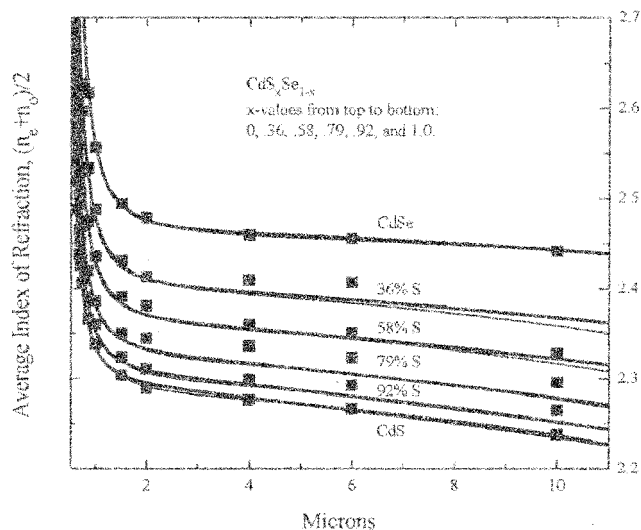


Fig. 3. Lisitsa's experimental data [21], represented by boxes, compared with indices predicted from the data for CdS and CdSe. The thick line was calculated using the relation $n(x, \lambda) = m(\lambda)x + b(\lambda)$. The thin line (largely occluded) was calculated by a weighed average of the Sellmeier coefficients. Data and calculations are presented for $\text{CdS}_x\text{Se}_{1-x}$, for x values of (from top to bottom): 0, .36, .58, .79, .92, and 1.0.

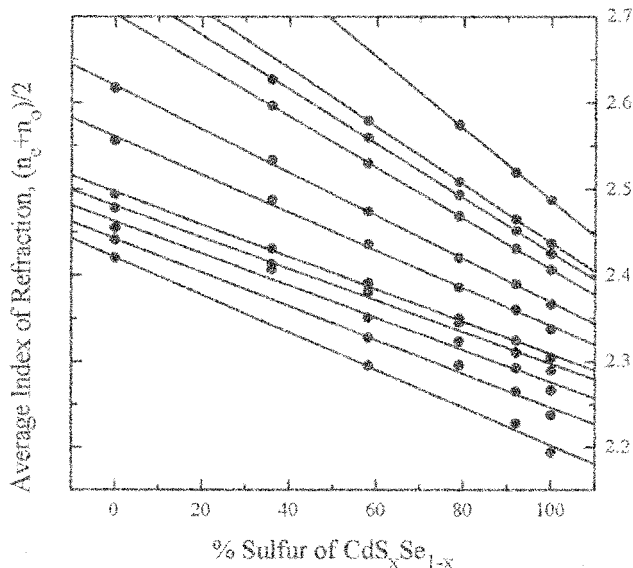


Fig. 2. The average index of refraction, $(n_e + n_o)/2$, of $\text{CdS}_x\text{Se}_{1-x}$, at a particular wavelength, as a function of sulfur concentration, according to the data of Lisitsa et al [21]. The lines in the graph are fit to the average index of refraction for wavelengths of (from top to bottom) .61 μm , .67 μm , .69 μm , .70 μm , .85 μm , 1.0 μm , 1.5 μm , 2.0 μm , 6.0 μm , 10.0 μm , and 14.0 μm .

of the Sellmeier equations:

$$n^2 = p_1 + \frac{p_2 \lambda^2}{(\lambda^2 - p_3)} + \frac{p_4 \lambda^2}{(\lambda^2 - p_5)} \quad (4)$$

The coefficients we found by fitting Lisitsa's data for CdS and CdSe are summarized in Table I. The results of both methods are presented in Fig. 3. Predictably, both methods showed excellent agreement with the CdS and CdSe data from which they were derived. At intermediate values of x , the methods agree well with each other for wavelengths shorter than 5 μm . For longer wavelengths, the method of averaging the Sellmeier coefficients gives a lower calculated value for the index than that obtained from the linear dependence of the index on the composition at a given wavelength, which is also closer to the actual data values. However, both methods underestimate the index of intermediate values of x , the greatest deviation being almost 1% at 4 μm for $\text{CdS}_{0.79}\text{Se}_{0.21}$. A slight plateau between 2–5 μm in the index of the intermediates, which is absent from the binaries, is not reproduced by either of the two methods.

THE BIREFRINGENCE OF THIS ALLOY SYSTEM

Birefringences of CdS and CdSe have also been published in conjunction with index measurements by a number of authors,^{8,18–22} and alloy-birefringence data is available from Lisitsa et al.'s work.²¹ However, when compared to one another, serious discrepancies are apparent in the reported values for CdS (Fig. 4). To assess the quality of these published

Table I. Parameters for the Three-Term Sellmeier Derived from Lisitsa's Data

Material	P_1	P_2	P_3	P_4	P_5
CdS	3.65416	1.54627	0.14603	21.32848	10,983.93238
CdSe	4.6696	1.36752	0.2689	1.02932	1,437.79278

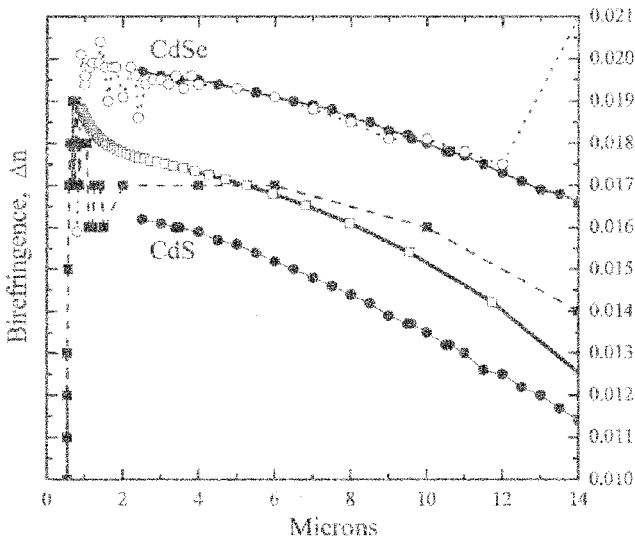


Fig. 4. The birefringence of CdS and CdSe, as reported by [8, 18–22]:

- Chenault [11] for CdS and CdSe
- Bond [10], Herbst [12], and Lisitsa [13] for CdSe
- Bieniewski [9] and Lisitsa [13] for CdS
- This Study, CdS₂Se_{0.8}

The birefringence we measured for CdS₂Se_{0.8} is in best overall agreement with the data of Chenault et al [20].

results, we measured the birefringence of a CdS_xSe_{1-x} single crystal of nominal composition $x = 0.2$, which was grown by one of us (Burger). To make this measurement, we employed the familiar cross-polarizer method.²³

In the crossed-polarizer technique, the sample is placed between two polarizers, both oriented at 45° to the crystal's optical axis. The resulting transmission spectrum displays an interference pattern (Fig. 5). The wavelengths at which the peaks in transmission

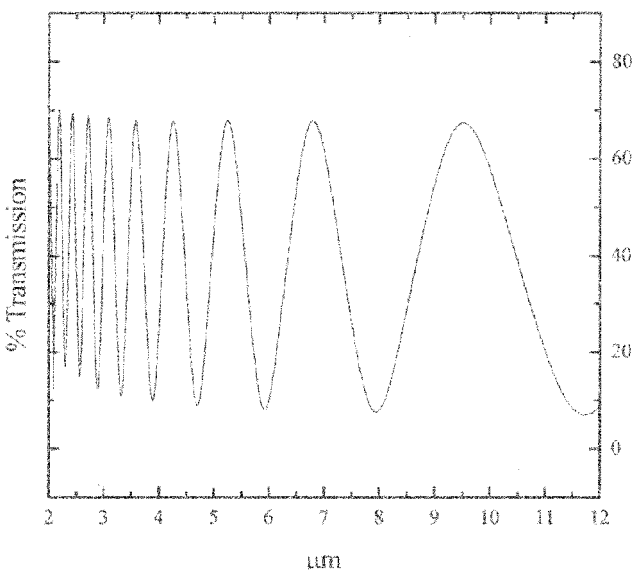


Fig. 5. The transmission spectrum of single crystal CdS₂Se_{0.8}:V, 1.222 mm thick, situated between two polarizers, both at 45° to the crystal's optical axis. The spectrum displays interference fringes.

occur are simply related to the value of the birefringence at that wavelength, according to the relation

$$\Delta n(\lambda) = \frac{i\lambda}{t} \quad (5)$$

where $\Delta n(\lambda)$ is the birefringence, λ is the wavelength at which the interference-fringe maximum occurs, t is the crystal thickness, and i is the order of the interference fringe. Determining the fringe order of each peak maximum may be accomplished by comparing the resultant birefringence with that of a known standard, whose birefringence was hoped to be close to that of the crystal in question. However, we have employed a simple protocol by which the order number can be determined unambiguously from a single sample.

First, an entire family of possible birefringence versus wavelength curves are generated from the interference data by successively incrementing the assumed fringe order number of the lowest observed fringe from 1–30. One of the curves in this family is likely to represent the true birefringence, the others being based on a false assumption. Next, the crystal is thinned by a noninteger fraction, and the process repeated. When the two families of curves are compared, the true birefringence is indicated by the two curves, which agree, while all other curves should fail to overlap. The birefringence we measured with this method is included in Fig. 4 and is clearly most consistent with the data of Chenault and Chipman,²⁰ as its values are intermediate between those of CdS and CdSe as expected.

To determine the compositional dependence of the birefringence, we again exploited the linear dependence of the indices for a particular wavelength on the composition. This time, we sought the wavelength dependence of the two parameters of the linear equation

$$\Delta n_\lambda = m'x + b' \quad (6)$$

where

$$\Delta n_\lambda = n_e - n_o \quad (7)$$

n_e is the extraordinary ray, and n_o is the ordinary ray. We determined the values of the slopes, m' , and y intercepts, b' , of these linear relationships by analyzing Chenault's data, using the same methodology we employed for the indices, and the results are displayed in Fig. 6. In Fig. 7, we see the birefringences of CdS and CdSe at several different wavelengths and the birefringence of our sample as well. The data highly suggests that the composition of our sample is actually closer to $x = 0.6$. Although we were not able to confirm this independently, this does suggest a simple way of determining the composition of an alloy from this optical measurement.

Using the functional dependencies of m and b derived from our analysis of Lisitsa's data, we calculated

$$n_{av} = (n_e + n_o)/2 \quad (8)$$

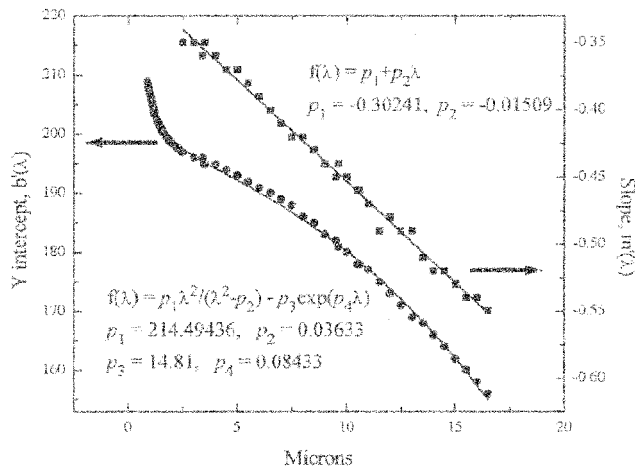


Fig. 6. The slopes and y-axis intercepts of the linear curves which relate the birefringence to composition, as a function of wavelength. The curves shown here give us $m'(\lambda)$ and $b'(\lambda)$ in the equation $\Delta n(x, \lambda) = m'(\lambda)x + b'(\lambda)$.

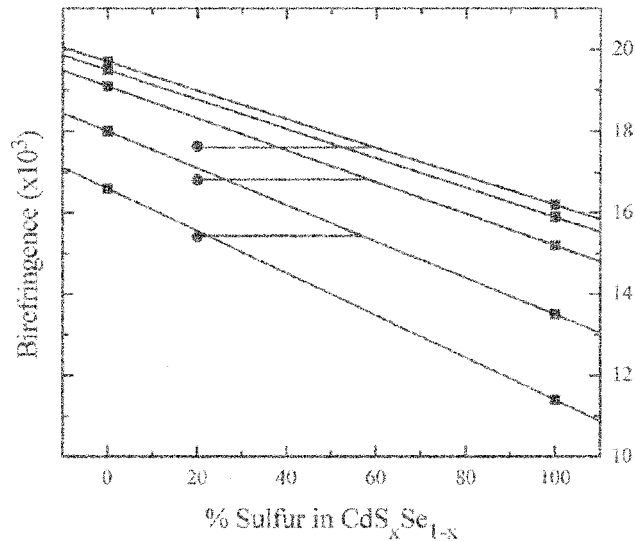


Fig. 7. The birefringences of CdS, CdSe, and our sample of CdS_xSe_{1-x} , of nominal composition $x = .2$. The birefringences of CdS and CdSe are given for wavelengths of (from top to bottom) 2.5 μm , 4 μm , 6 μm , 10 μm , and 14 μm . The birefringence of our crystal is given for (from top to bottom) 2.5 μm , 6 μm , and 10 μm . The graph suggests that the true composition of our compound is closer to $x = .6$.

for $x = 0-1$ in increments of 0.1. From the m' and b' , we calculated from Chenault's data, we found Δn for the same values of x .

Finally, we calculated the Type I second-harmonic generation phase-matching angle for this alloy system, using the equations¹³

$$n(\lambda)_e = n(\lambda)_{av} + \Delta n(\lambda) \quad (9)$$

$$n(\lambda)_o = n(\lambda)_{av} - \Delta n(\lambda) \quad (10)$$

$$\sin^2 \theta = \frac{(n_e/n'_o)^2 \{ (n'_o + n_o)(n'_o - n_o) / (n_e + n_o)(n_e - n_o) \}}{\quad} \quad (11)$$

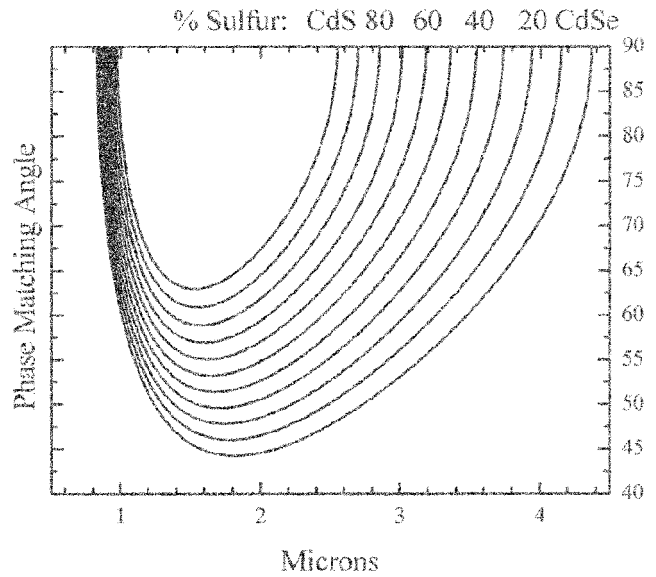


Fig. 8. Phase matching curves for CdS_xSe_{1-x} . Angles for phase matching at 2 microns are:

% Sulfur	Angle	% Sulfur	Angle
0	44.549	60	57.057
10	46.528	70	59.393
20	48.534	80	61.862
30	50.576	90	64.504
40	52.668	100	67.385
50	54.822		

The results, presented in Fig. 8, reveal that noncritical phase matching should be possible with these alloys from 2.55 μm to 4.35 μm .

IMPURITY ABSORPTION AND PHOTOLUMINESCENCE

The transmission spectrum of $CdS_{0.2}Se_{0.8}:V$ displays three broad peaks close to the absorption band edge of energies 0.979 eV, 1.087 eV, and 1.181 eV at 24 K (Fig. 9). These peaks are entirely absent from a sample of undoped $CdS_{0.2}Se_{0.8}$, leading us to assign the peaks to the vanadium dopant. These peaks did not show appreciable polarization sensitivity nor did they sharpen when the sample was cooled to 15 K. However, the peak position did shift with the change in temperature. Specifically, the middle peak remained essentially constant, while the higher energy peak moved to higher energy, and the lower energy peak moved to lower energy. Thus, at 15 K, the high- and low-energy peaks are both separated from the middle peak by 100 meV, while at room temperature, they are both 150 meV distant from the middle peak (Fig. 10). This temperature dependence and the energies of the peaks would be consistent with the 0.98-eV peak being caused by a 3A to 1E transition, and the other two peaks caused by 3A to 3d1 transitions within the V^{3+} ion.

Similarly, the photoluminescence spectrum shows an emission peak at 1.8 eV, which is absent from the undoped sample, that we also assign to the vanadium

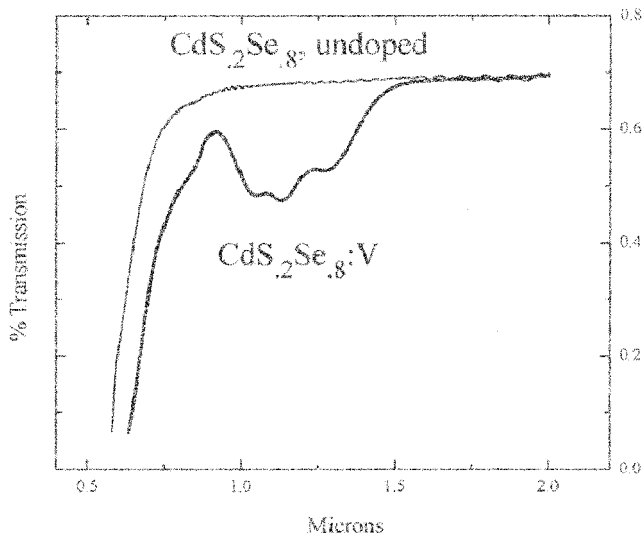


Fig. 9. The near-band-edge impurity absorption bands of CdS_{0.2}Se_{0.8}:V. The thick line is CdS_{0.2}Se_{0.8}:V, while the thin line is undoped CdS_{0.2}Se_{0.8}.

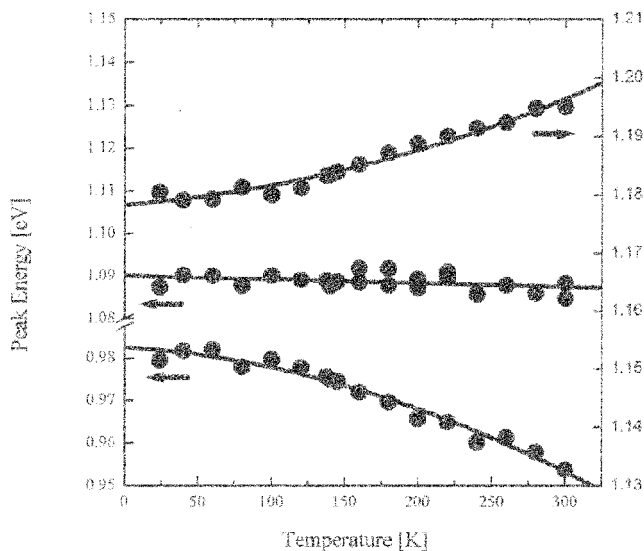


Fig. 10. The location of the peaks of the impurity band with temperature. The high energy peak moves to higher energies with increasing temperature, and the low energy peak moves to lower energies, while the mid-energy peak remains relatively stationary.

dopant. An exciton peak is observed in the photoluminescence spectrum at 2.240 eV, with phonon replicas at 2.276 eV and 2.308 eV. In addition, there is an emission peak at 1.45 eV, which is common to both the doped and the undoped samples.

CONCLUSIONS

We have reviewed the literature data for the indices of refraction of CdS_xSe_{1-x} alloys and discover a linear relationship between alloy composition and index at a particular wavelength. We have compared the results of calculating the alloy index by averaging Sellmeier coefficients with the results obtained by exploiting this empirical relationship. The methods agree well with each other for wavelengths shorter

than 5 μm. For longer wavelengths, the method of averaging the Sellmeier coefficients gives a lower calculated value for the index than that obtained from the linear dependence of the index on the composition at a given wavelength, which is also closer to the actual data values. Furthermore, features at intermediate values of x, absent from the endpoint data, are not reproduced by either of the estimates.

The same approach was used to calculate the compositional dependence of the birefringence, and the two results combined to calculate the Type-I second-harmonic generation phase-matching angles for different alloy compositions. The results reveal that it should be possible to achieve noncritical phase matching of these alloys from 2.55 μm to 4.35 μm.

The transmission and photoluminescence spectra of CdS_{0.2}Se_{0.8}:V were compared to that of the undoped alloy. Three transmission peaks (at 0.979 eV, 1.087 eV, and 1.181 eV) and one photoluminescence peak (at 1.8 eV) were present in the doped sample and absent in the undoped sample.

ACKNOWLEDGEMENTS

This research was supported by NSF Grant No. HRD-9550605 and U.S. Air Force Grant No. GYF1457096-03120.

REFERENCES

1. T.H. Allik, S. Chandra, D.M. Rines, P.G. Schunemann, J.A. Hutchinson, and R. Utano, *Opt. Lett.* **22**, 597 (1997).
2. T. Allik, S. Chandra, D. Rines, P. Schunemann, J.A. Hutchinson, and R. Utano, *Advanced Solid State Lasers*, ed. C.R. Pollock and W.R. Bosenberg (Washington, DC: Optical Society of America, 1997), pp. 265–266.
3. K. Chattopadhyay, K.M. Pour, S.U. Egariyev, J.O. Ndap, H. Chen, X. Ma, S. Morgan, and A. Burger, *J. Electron. Mater.* **28**, 666 (1999); D.S. Bethune and A.C. Luntz, *Appl. Phys. B* **40**, 107 (1986).
4. G.C. Bhar, D.C. Hanna, B. Luther-Davies, and R.C. Smith, *Opt. Commun.* **6**, 323 (1972).
5. A.A. Davydov, L.A. Kulevskii, A.M. Prokhorov, A.D. Savel'ev, V.V. Smirnov, and A.V. Shirkov, *Opt. Commun.* **9**, 234 (1973).
6. A. Dhirani and P. Guyot-Sionnest, *Opt. Lett.* **20**, 1104 (1995).
7. D.C. Hanna, B. Luther-Davies, R.C. Smith, and R. Wyatt, *Appl. Phys. Lett.* **25**, 142 (1974).
8. R.L. Herbst and R.L. Byer, *Appl. Phys. Lett.* **19**, 527 (1971).
9. R.L. Herbst and R.L. Byer, *Appl. Phys. Lett.* **21**, 189 (1972).
10. J.A. Weiss and L.S. Goldberg, *Appl. Phys. Lett.* **24**, 389 (1974).
11. R.G. Wenzel and G.P. Arnold, *Appl. Opt.* **15**, 1322 (1976).
12. S.H. Morgan, M. Davis, Z. Pan, K.-T. Chen, H. Chen, S.L. Davis, and A. Burger (Paper presented at the Materials Research Society Spring Meeting, San Francisco, CA, 13–17 April 1997).
13. V.G. Dmitriev, G.G. Gurzadyan, and D.N. Nikogosyan, *Handbook of Nonlinear Optical Crystal*. 2nd ed. (Berlin: Springer, 1997).
14. L.M. Hoang and J.M. Baranowski, *Phys. Status Solidi (b)* **84**, 361 (1977).
15. R. Pappalardo and R.E. Dietz, *Phys. Rev.* **123**, 1188 (1961).
16. J.M. Langer and J.M. Baranowski, *Phys. Status Solidi (b)* **44**, 155 (1971).
17. D. Buhmann, J.-J. Schulz, and M. Thiede, *Phys. Rev. B* **19**, 5360 (1979).

18. T.M. Bieniewski and S.J. Czyzak, *J. Opt. Soc. Am.* 53, 496 (1963).
19. W.L. Bond, *J. Appl. Phys.* 36, 1674 (1965).
20. D.B. Chenault and R.A. Chipman, *Appl. Opt.* 32, 4223 (1993).
21. M.P. Lisitsa, L.F. Gudymenko, V.N. Malinko, and S.F. Terekhova, *Phys. Status Solidi (b)* 31, 389 (1969).
22. M. Schaffner, X. Bao, and A. Penzkofer, *Appl. Opt.* 31, 4546 (1992).
23. R.W. Ditchburn, *Light* (London: Interscience, 1963).